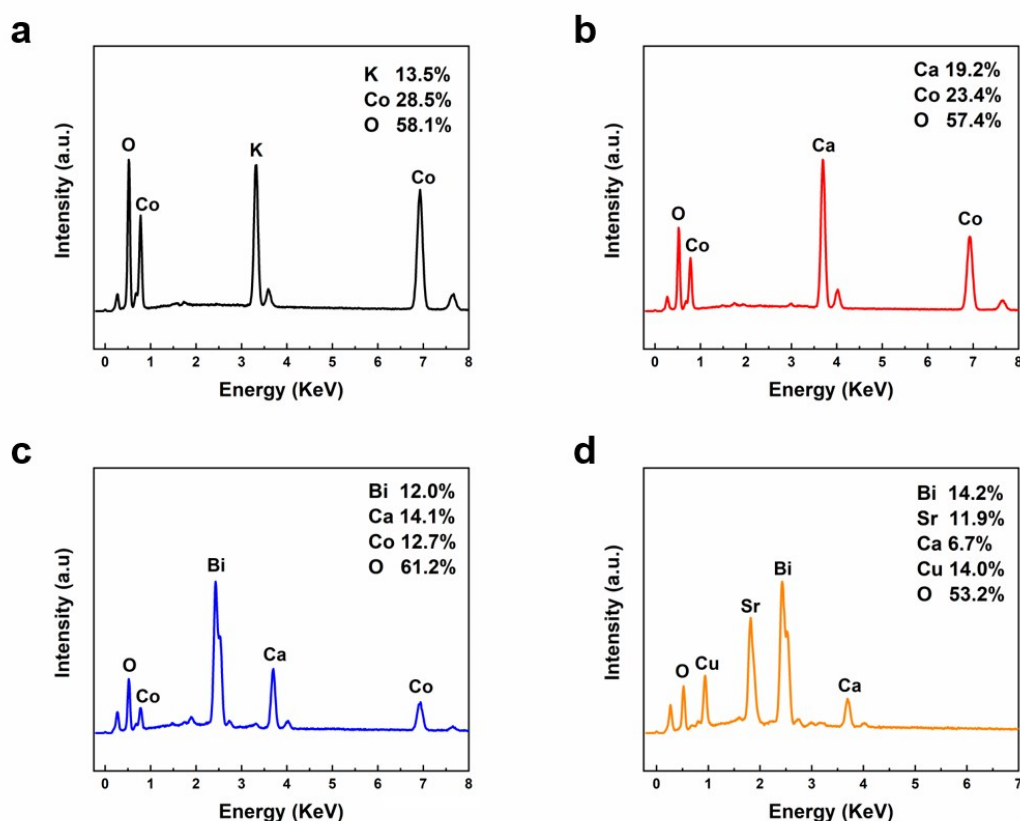


## 1. Sample Characterizations:

All the samples investigated in this paper were synthesised by flux method and detailed information about the crystal growth has been described in this paper and previous studies<sup>1</sup> already. Structural characterizations including energy dispersion spectrum (EDS), X-Ray diffraction (XRD) and Raman spectrum were carried out and most of the results have been shown in the paper. EDS results of all the samples are shown in **Figure S1**. The stoichiometric ratio is  $K_{0.5}CoO_2$  for KCO,  $Ca_3Co_4O_9$  for CCO,  $Bi_{1.85}Ca_2Co_{1.85}O_{8.75}$  for BCCO and  $Bi_2Sr_2CaCu_2O_9$  for BSCCO. Extra oxygen atoms are usually added between the BiO layers.



**Figure S1.** Energy dispersion spectra of (a)KCO, (b)CCO, (c)BCCO and (d)BSCCO.

Cross-section transmission electron microscopy was performed on BCCO to examine the crystal quality. The micrograph is shown in **Figure S2**. Layered lattice

structure without obvious disorder can be seen from the image and the dotted electron diffraction pattern along the  $c$ -axis proves the absence of cross-plane disorder. Misfit interfaces are clearly visible from the figure. Although van der Waals interfaces are not clearly seen, from previous reports and our experimental results their influence is pronounced.

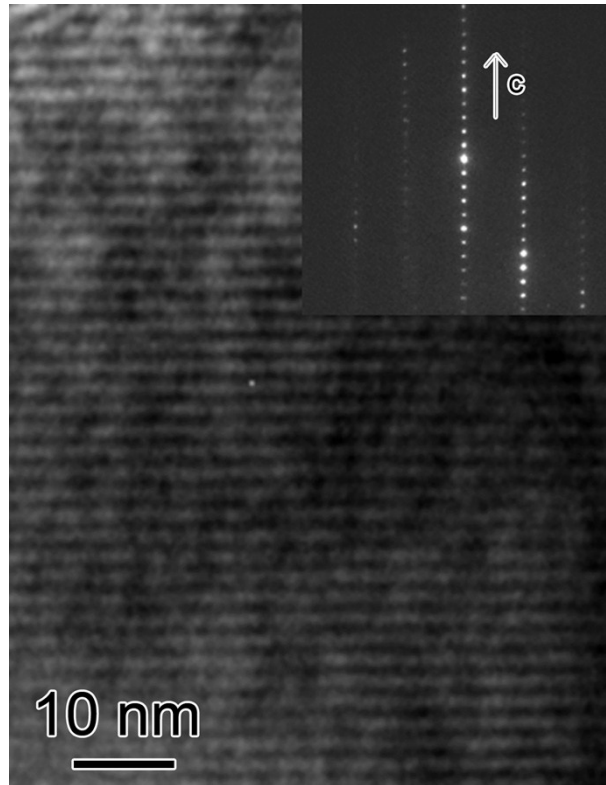


**Figure S2.** Cross-section transmission electron microscopy image of BCCO. The inset shows the electron diffraction pattern along the  $c$ -axis.

## 2. Time-Domain ThermoReflectance:

Time-domain thermoreflectance (TDTR) measurements were carried out to measure the cross-plane thermal conductivity of the samples. The samples were mounted onto silicon substrates by silver paste and a  $\sim 80$  nm aluminium film was deposited by magnetron sputtering to serve as a heat transducer. Before the deposition all the samples were mechanically exfoliated by scotch tapes to get clean and fresh

surfaces. A femtosecond pulsed laser with 770nm-centered wavelength was used in the measurements and was split into two beams with a power ratio of 2:1 (14mW for pump beam and 7mW for probe beam). More detailed information about our system could be found in our previous studies.<sup>2,3</sup>

Ratio sensitivity ( $S_\alpha$ ) is widely used in the TDTR data analysis to denote how sensitive are the signals to specific physical parameter  $\alpha$  (such as thermal conductivity, volumetric heat capacity and thickness of each layer). It is defined as:

$$S_\alpha = \frac{\partial \ln(-V_{in}/V_{out})}{\partial \ln(\alpha)}$$

A higher sensitivity means the signal is more sensitive to a tiny change of the certain parameter. In order to insure a higher accuracy of the measurements, we expect that the sensitivity of the sample thermal conductivity should be a relatively high value. Ratio sensitivity of the parameters at ambient temperature were calculated and shown in **Figure S3**. Here, Al represents aluminum film, interface is the interface between aluminum and sample, and sample is the materials investigated. It is proved that the measurements are sensitive to the cross-plane thermal conductivity and capacity heat of the sample and the thickness and capacity heat of the aluminum film. Here, thickness of the aluminum film was measured by picosecond laser ultrasonics, which has been illuminated in the paper. The capacity heat of both aluminum film and samples were extracted from the literature.<sup>4,5,6,7</sup> In that case we estimate a ~9% systemic error in the TDTR measurements.

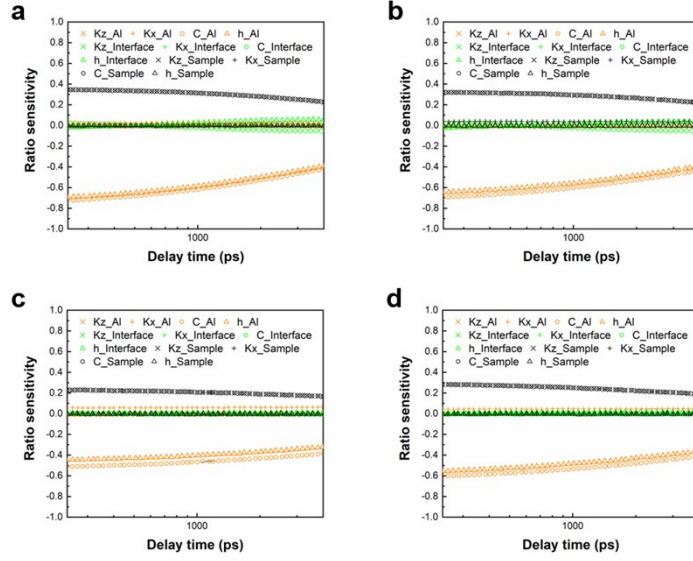


**Figure S3.** Sensitivity plots of (a) KCO, (b) CCO, (c) BCCO and (d) BSCCO.

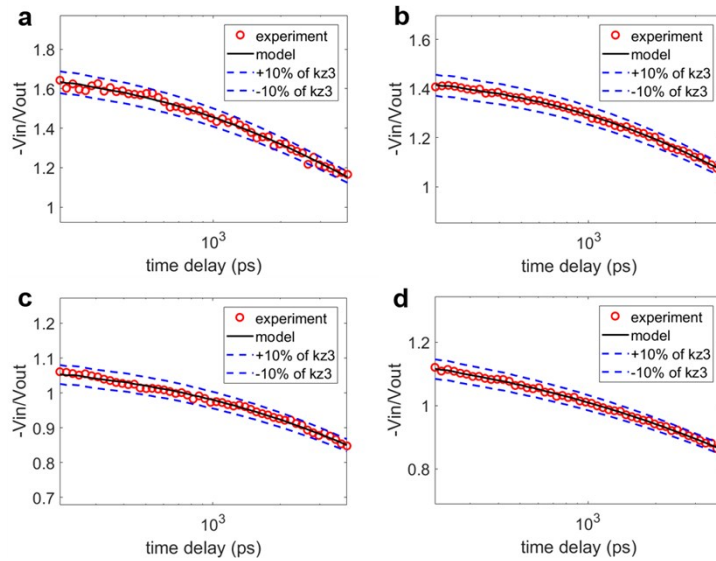


**Figure S4.**  $-V_{in}/V_{out}$  plots of (a)KCO, (b)CCO, (c)BCCO and (d)BSCCO measured by TDTR at room temperature. The black solid lines represent optimal fitting to the data while the blue dashed lines represent the condition when a range of  $\pm 10\%$  error is considered.

Thermal conductivity of the investigated crystals are close to the lattice thermal

conductivity. Here we take CCO as an example. In-plane electrical and thermal properties of CCO have been reported.<sup>8</sup> At 300 K, the in-plane  $\sigma$  is  $5 \times 10^4 \Omega^{-1} \text{ m}^{-1}$ . According to the Wiedemann-Franz's law and taking the Lorenz factor  $L_0$  as  $2.45 \times 10^{-8} \text{ W } \Omega \text{ K}^{-2}$ , the in-plane  $\kappa_e$  can be calculated by  $\kappa_e = \sigma L_0 T$  to be  $\sim 0.3675 \text{ W m}^{-1} \text{ K}^{-1}$ . Considering the anisotropy nature of lattice, we assume the cross-plane  $\kappa_e$  to be a factor of 5 lower, about  $0.0735 \text{ W m}^{-1} \text{ K}^{-1}$ . In that case, electrons contribute  $\sim 5\%$  to the cross-plane thermal conductivity. Therefore, the thermal conductivity can be viewed as lattice thermal conductivity.

### 3. Picosecond Laser Ultrasonics:

Measurements of picosecond laser ultrasonics (PLU) were performed to characterize the cross-plane acoustic velocities of the samples. Detailed information about PLU has been interpreted in the paper. Five KCO flakes and four CCO flakes were measured, and all the results has been presented in the paper. **Figure S5** and **Figure S6** shows the results for all the individual flakes. In most of the cases there are only two echos, while in some cases there is a secondary reflection of the acoustic wave at the aluminum-flake interface, forming another echo at two-fold delay time of the first echo. Such a difference should be owing to the variation in quality of the interface, which is beyond the scope of this paper.

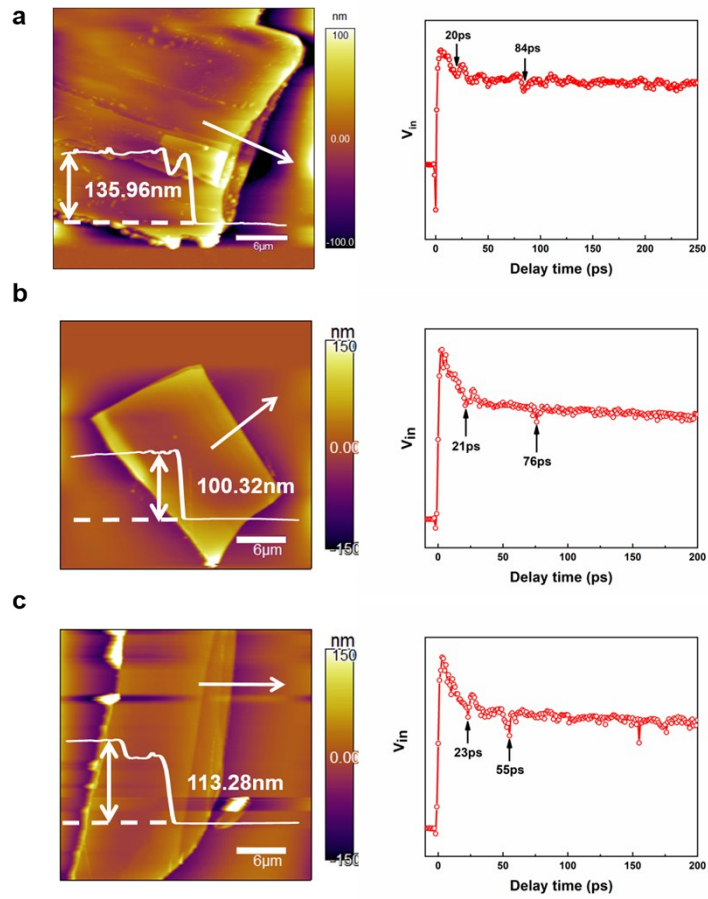


**Figure S5.** Atomic force microscope images and echo signals collected for all the CCO flakes by PLU

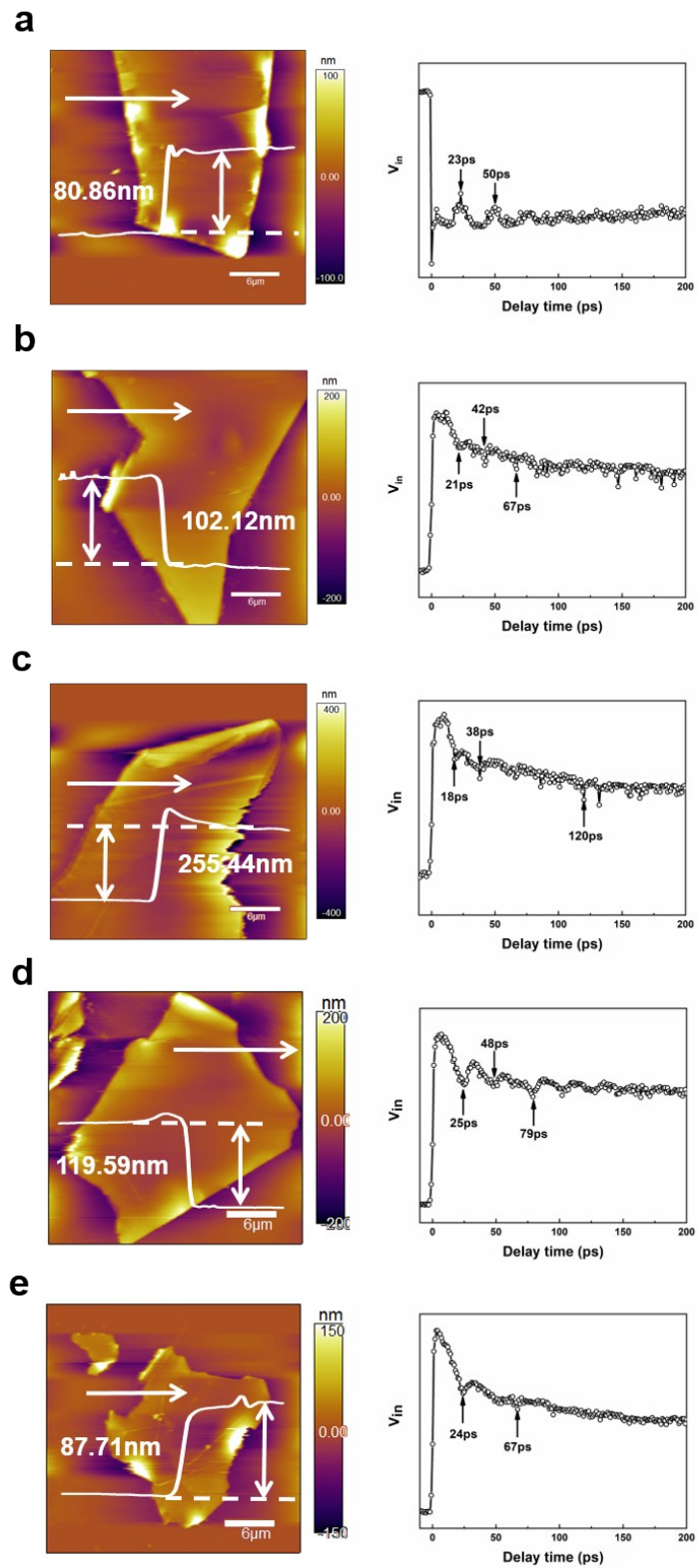


**Figure S6.** Atomic force microscope images and echo signals collected for all the KCO flakes by PLU

## References:

1. S. T. Dong, B. B. Zhang, Y. Xiong, Y. Y. Lv, S. H. Yao, Y. Chen, J. Zhou, S. T. Zhang and Y. F. Chen, *Journal of Applied Physics*, 2015, **118**, 125108.
2. X. J. Yan, Y. Y. Lv, L. Li, X. Li, S. H. Yao, Y. B. Chen, X. P. Liu, H. Lu, M. H. Lu and Y. F. Chen, *npj Quantum Mater.*, 2017, **2**, 31.
3. X. J. Yan, Y. Y. Lv, L. Li, X. Li, S. H. Yao, Y. B. Chen, X. P. Liu, H. Lu, M. H. Lu and Y. F. Chen, *Appl. Phys. Lett.*, 2017, **110**, 211904.
4. J. Wooldridge, D. M. Paul, G. Balakrishnan and M. Lees, *J. Phys.: Condens. Matter*, 2005, **17**, 707.
5. A. Rébola, R. F. Klie, P. Zapol and S. Ötüt, *Appl. Phys. Lett.*, 2014, **104**, 251910.
6. O. Jankovský, D. Sedmidubský, K. Rubešová, Z. Sofer, J. Leitner, K. Rušička and P. Svoboda, *Thermochim. Acta*, 2014, **582**, 40.
7. H. Kierspel, H. Winkelmann, T. Auweiler, W. Schlabitz, B. Büchner, V. Duijn, N. Hien, A. Menovsky and J. Franse, *Physica C: Superconductivity*, 1996, **262**, 177.
8. M. Shikano and R. Funahashi, *Appl. Phys. Lett.*, 2003, **82**, 1851.